Title: Properties of neutron doped multicrystalline silicon for solar cells

Author: C. Pochrybniak, K. Pytel, J. J. Milczarek, J. Jaroszewicz, M. Lipiński, T. Piotrowski, Jerzy Kansy

Citation style: Pochrybniak C., Pytel K., Milczarek J. J., Jaroszewicz J., Lipiński M., Piotrowski T., Kansy Jerzy. (2008). Properties of neutron doped multicrystalline silicon for solar cells. "Acta Physica Polonica A" (Vol. 113, iss. 4 (2008), s. 1255-1265), doi 10.12693/APhysPolA.113.1255

Proceedings of the National Conference on Neutron Scattering and the Complementary Methods in the Investigations of the Condensed Phases, Chlewiska 2007

Properties of Neutron Doped Multicrystalline Silicon for Solar Cells

C. Pochrybniak[a,*], K. Pytel[a], J.J. Milczarek[a], J. Jaroszewicz[a], M. Lipiński[b], T. Piotrowski[c] and J. Kansy[d]

[a]Institute of Atomic Energy, Świerk, 05-400 Otwock, Poland
[b]Institute of Metallurgy and Materials Science
Polish Academy of Sciences
Reymonta 25, 30-059 Cracow, Poland
[c]Institute of Electron Technology, Warsaw, Poland
[d]University of Silesia, Bankowa 12, 40-007 Katowice, Poland

Dedicated to Professor Jerzy Janik on the occasion of his 80th birthday

The technology of neutron transmutation doping of silicon wafers in MARIA nuclear research reactor is described. The studies of the radiation defects performed with positron annihilation confirmed that divacancies dominate in the irradiated material. Thermal treatment of irradiated silicon at 700−1000°C produces void–phosphorus complexes and void aggregates. The resistivity of the samples produced by neutron transmutation doping was found to be uniform within 2.5% limits. The severe reduction of the minority carrier lifetime in irradiated samples was confirmed.

PACS numbers: 81.40.Wx, 71.60.–i, 78.70.Bj, 61.80.–x

1. Introduction

Due to the complexity of solar grade multicrystalline silicon its physical properties are interesting field of research of modern materials engineering [1]. During crystallization process, contaminations aggregate in liquid phase of silicon and precipitate at the borders of grains. Therefore, their presence determines the quality of multicrystalline material. They host the centers of recombination that decrease minority carrier's lifetime [2, 3]. One of the main problems during silicon crystallization is spatial homogeneity of the dopant distribution, which decides on the type of electrical conductivity and value of specific resistivity of

*corresponding author; e-mail: c.pochrybniak@cyf.gov.pl

material. Useful level of the dopant concentration in silicon ranges from 10^{15} to 10^{16} cm^{-3} [4]. The differences in specific resistivity in the sample reach several percent, after traditional doping in silicon crystallization process. Metallic contaminations, "lifetime killers" of minority carriers, are in solar grade silicon at the level of $10^{11}-10^{13}$ cm^{-3}. Since the resistivity of silicon for solar cell should be 0.5–10 Ω cm, the concentration of the dopant atoms must be at 10^{15} to 10^{16} cm^{-3}. Gettering the parasitic contaminations and passivation of recombination centers requires additional thermal processes. However, intensive thermal processes of multicrystalline silicon decrease the mobility of minority carriers and reduce their lifetime.

Basic nuclear reaction employed in the neutron transmutation doping (NTD) of silicon consists in transformation of silicon nuclei to phosphorus ones after capture of thermal neutron

$$^{30}_{14}\mathrm{Si}(\mathrm{n},\gamma)^{31}_{14}\mathrm{Si} \quad \stackrel{2.62\ \mathrm{h}}{\longrightarrow} \quad ^{31}_{15}\mathrm{P} + \beta^{-}.$$

The reaction is used mainly in production of semiconductor power circuits and γ-ray detectors. The non-uniform spatial distribution of dopant in irradiated sample of Si is due to the self-shielding effect and is not a problem even for large crystals.

During irradiation the crystal defects are produced in transmutation of silicon. Defects can be removed by thermal annealing processes in the solar cells manufacturing. It is expected that the basic merits of NTD, i.e. spatial homogeneity and small phosphorus concentration between borders of grains in basic material, will improve solar cells parameters.

In Sect. 2 we give a short description of the implementation of NTD technique in MARIA reactor. The samples are described in Sect. 3. The results of positron annihilation studies of the defects introduced by radiation are presented in Sect. 4.1. The distribution of resisitivity across samples is presented in Sect. 4.2.

2. NTD procedure

In order to obtain appropriate concentration of phosphorus in reasonable time, the high thermal neutron flux density is needed. The resistivity below 1 Ω cm can be reached in 100 h with the thermal neutron flux density of 10^{14} cm^{-2} s^{-1}. This flux density is met in the core of the nuclear research reactor MARIA in the vicinity of fuel elements, at first row of the beryllium reflector. The necessary irradiation conditions are provided in Ø60 irradiation channel in beryllium block denoted as J-IX in the reactor core matrix.

Before irradiations the thermal neutron flux density and epithermal index were determined. As activation detectors foils of alloys of gold with aluminum and cobalt were used. The determined total neutron flux density was 1.0×10^{14} cm^{-2} s^{-1} $\pm$ 4.8%, and epithermal index was 0.05 ± 0.02. The determined epithermal index indicates that there is appreciable fraction of the fast neutrons in the total neutron flux present. One should expect that the fast neutrons

might generate high density of radiation defects within the bulk of the irradiated material.

Distribution of thermal neutron flux density along the axis of the irradiation channel was determined by the copper wire activation method. The distribution exhibits marked maximum at 660 mm depth from upper edge of beryllium block. In the 100 mm region containing that maximum the neutron flux density is almost constant within 2%. The size of the region matches the sample height. The self--shielding effect of silicon estimated from distribution of neutron flux density in the neutron reflector region yields for 2 inch diameter samples the 5 to 8% radial differences in doping. In order to decrease this effect, the samples should be rotated around vertical axis during the irradiation.

3. Samples

Silicon wafers cut from floating-zone method produced single-crystalline and multicrystalline materials of 500–800 Ω cm resistivity were used. The wafers were of 2 inch diameter and 0.5 mm thick disks. Two series differing in irradiation time were carried out. The thermal neutron dose for the irradiated samples was determined with special activation detectors (foil AlCo) placed between samples. The expected resistivity after irradiation of the silicon was estimated from the determined neutron dose by standard procedure [5].

For the first set of samples, irradiated for 100 h, the values of thermal neutron dose and expected resistivity were

activation detector No. 1 $\quad 3.4 \times 10^{19}$ cm^{-2} $\quad \rho = 0.77$ Ω cm,

activation detector No. 2 $\quad 3.7 \times 10^{19}$ cm^{-2} $\quad \rho = 0.72$ Ω cm,

determined with the error of 5.2% in both cases.

For the second set of samples, irradiated for 42 h the neutron dose and expected resistivity were

activation detector No. 3 $\quad 1.31 \times 10^{19}$ cm^{-2} $\quad \rho = 2$ Ω cm,

and the error of measurement was 2.5%.

The silicon samples were "cooled" during the week after irradiation. Only slim contaminations from the second circulation of reactor cooling water were noticed, i.e. ^{46}Sc, ^{51}Cr, ^{103}Ru, and ^{141}Ce. After standard cleaning the samples in special acid bath (mixture of citrates and citric acid) and ultrasonic cleaning in water bath, most of contaminations (more than 95%) were removed.

4. Results

The radiation defects introduced into the samples by the nuclear radiation were studied with the positron annihilation. The main part of studies dealt with the single-crystalline samples, because it is not reasonable to compare the defects in different samples of the multicrystalline silicon. The single-crystalline samples

provide appropriate uniformity of initial material needed for comparison of the radiation defects. It is assumed that the radiation defect density is the same in single- and multicrystalline samples. For comparison the not irradiated silicon samples with resistivity about 1 kΩ cm (undoped) and 5 Ω cm (doped during crystallization) and irradiated samples were investigated.

4.1. Radiation deffects

Positron lifetime measurements were made at room temperature with the conventional fast-fast spectrometer of the time resolution of 270 ps for Co-60. The positron source of activity about 740 kBq, covered by 5 μm Ni foil, was placed between two pieces of the investigated sample. 10 to 20 lifetime spectra were recorded for each sample. Then the spectra were added using the special procedure which accounted for the drift of the zero channel. With this procedure the very high counts ($30–60 \times 10^6$) were achieved.

The experimental data were analyzed with the LT-9 program [6] that unlike other codes used in the field, is suitable for fitting not only a single spectrum but also enables simultaneous fits to series of spectra. The simultaneous fitting of many spectra reduces the number of the free parameters if some of them are common for all analyzed spectra.

In our case the series composed of nine spectra each were collected for samples after different annealing procedures. The results were analyzed within the three-state trapping model [7, 8]. The model takes into account the processes of positron annihilation in the bulk material and at the two types of defects. Within the model the positron lifetime spectrum $S(t)$ consists of three components

$$S(t) = \sum_{j=0}^{2} I_j \lambda_j \exp(-\lambda_j t). \tag{1}$$

Parameters $\lambda_0 = 1/\tau_\mathrm{b} + \mu_1 c_1 + \mu_2 c_2$ and $\lambda_j = 1/\tau_j$ ($j = 1, 2$) denote the positron annihilation rates at bulk and different types of defects (Fig. 1), whereas I_j are intensities given by

$$I_0 = 1 - I_1 - I_2 \quad \text{and} \quad I_j = \frac{\mu_j c_j}{\lambda_0 - \lambda_j}, \quad j = 1,\ 2. \tag{2}$$

We assumed that the structure of the bulk material and the two types of defects does not change during different annealing procedures. Therefore, the positron lifetimes τ_b, τ_1, and τ_2 do not change with the temperature and duration of annealing. The τ_b, τ_1, and τ_2 were determined from fitting the formula (1) to all the spectra of investigated samples. Because annealing changes the defects' concentrations, the fit parameters $\mu_1 c_1$ and $\mu_2 c_2$ were assumed to be different for each sample.

It turned out that in order to obtain a good fit to the data, a long-lived component (about 2 ns) with the intensity lower than 1% had to be incorporated into the description of each spectrum. Moreover, a source correction (4.5% of 105 ps and 0.5% of 320 ps) was made.

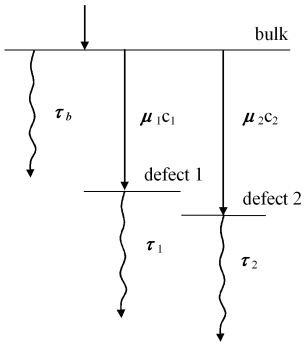

Fig. 1. The scheme of the positron annihilation processes according to the 3-state trapping model. The horizontal lines represent the free states of positron, i.e. the delocalized state of positron in the bulk of the material and its two localized states in two types of defects. τ_b is the positron lifetime in bulk material, τ_1 and τ_2 are the positron lifetimes in two different types of defects, respectively. $\mu_1 c_1$ and $\mu_2 c_2$ are the trapping rates into these defects, which are proportional to their concentrations c_1 and c_2.

The determined values of τ_b, τ_1, τ_2 and the long lifetime τ_3 obtained from the fitting are shown in Table I. The τ_b is lower by about 25 ps from the most frequently observed value of 218–220 ps for pure silicon [8–11]. Nevertheless, it is in the range of theoretical values (186 and 221 ps) predicted by different theoretical approaches [8].

TABLE I

The lifetimes of positron in the bulk (τ_b) and in two different defect states (τ_1 and τ_2) as well as the lifetime of the long-lived component (τ_3).

Sample (annealing [min], temperature [°C])	τ_b [ps]	τ_1 [ps]	τ_2 [ps]	τ_3 [ns]
(30',500), (30', 600)				1.52
(10', 700), (30', 700) (10', 800), (30', 800) (10', 900), (30', 900) (30', 1000)	193	295	266	2.25

The lifetime spectra of samples annealed for 30 min at 500°C and 600°C contain, in addition to a short-lived component originating from the positron annihilation in bulk, an additional one with the lifetime (τ_1) of 295 ps. Its relative intensity is 68% and 47% for 500 and 600°C, respectively. Since the lifetime pa-

rameter of this component is exactly the same as the one obtained for neutral divacancies in silicon at 300 K [12, 13] and the reported values of the positron lifetime for those divacancies in Si are contained in the range of 295–330 ps [8–13], it is evident that the component is due to the positron annihilation at neutral divacancies (V_2^0).

For the samples annealed at 700°C intensity of the component associated with V_2^0 decreases to 4.6% and 3.7% after 10 and 30 min of annealing, respectively. Additionally, in the lifetime spectra of these samples a new component of lifetime $\tau_2 = 266$ ps was found. We should mention that a component of similar lifetime of about 250 ps was found in NTD silicon samples [9, 11] and was ascribed to positron annihilation at E-type defects. The E-type defect is a complex (V–P) of a monovacancy and an atom of phosphorus. The theoretically calculated value of the positron lifetime in this type of defect is 270 ps [14] that is very close to our experimental result.

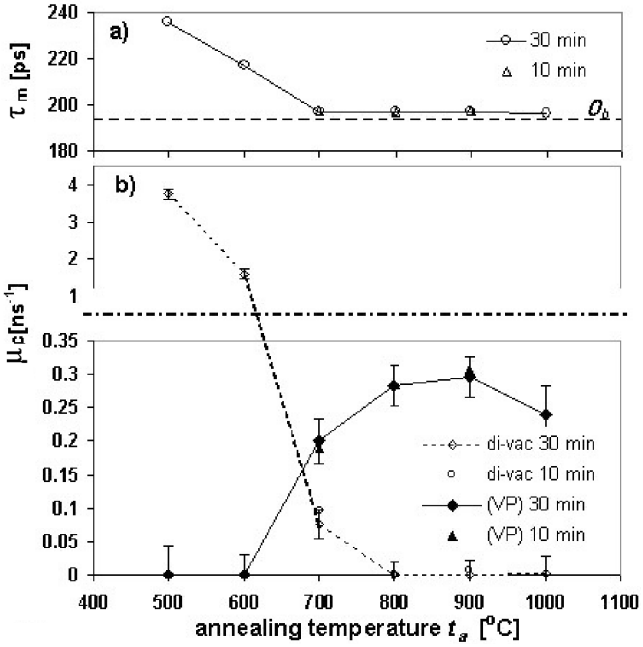

Fig. 2. (a) Mean positron lifetime τ_{m} in the investigated samples as a function of the annealing temperature (t_{a}) and annealing time (the error bars are hidden in the graphic symbols). The horizontal dashed line represents value of the bulk lifetime τ_{b}. (b) Dependence of the trapping rates into divacancies (open diamonds and circles) and into V–P complexes (solid circles and triangles) on the annealing temperature and time. Because the trapping rate into divacancies below $t_{\mathrm{m}} = 700$°C is much higher than that above this temperature, the graph is divided in two different scales.

For samples annealed at 800°C and 900°C the contribution of V_2^0 component disappears and the component due to annihilation at V–P complexes stabilizes at 17%, for any annealing time studied. For samples annealed at 1000°C part of E-type defects is removed yielding the decrease in the corresponding spectrum component to 14.5%.

The global changes in the positron lifetime spectrum are revealed in the behavior of the mean positron lifetime τ_m that is determined with high precision independently of the model used. We found that for our samples τ_m decreases drastically for annealing temperatures $t_m > 500$°C (Fig. 2a). The decrease can be easily explained as annealing of V_2 defects. Since the asymptotic value of τ_m is higher than τ_b, another type of defects should be present in samples annealed above 600°C. The evolution of the defect concentration in the investigated samples is described by the changes of the positron trapping rates $\mu_1 c_1$ and $\mu_2 c_2$ into V_2^0 and V–P complexes, respectively (Fig. 2b). The concentration of V_2 decreases sharply if the annealing temperature t_m exceeds 500°C. The V_2^0 defects practically disappear for $t_m > 700$°C. On the other hand, the V–P complexes are not observed for t_m below 600°C. They start to form in samples annealed at $t_m > 600$°C. Their concentration increases when the annealing temperature is increased up to $t_m \approx 900$°C and above this temperature it decreases gradually.

On the basis of the determined positron trapping rates the concentrations of discussed defects were estimated (Table II) using the positron trapping constants for V_2^0 ($\mu_1 = 1.5 \times 10^{-8}$ cm^3 s^{-1} [15]) and $(V–P)^0$ ($\mu_2 = 1.4 \times 10^{-8}$ cm^3 s^{-1} [16]).

TABLE II

Estimated values of V_2^0 and V–P concentration after anealing of samples for 10 and 30 min at different temperatures.

Annealing time [min]	Annealing temperature [°C]	Concentration V_2^0 (c_1) [cm^{-3}]	Concentration V–P (c_2) [cm^{-3}]
30	500	2.5×10^{17}	$> 10^{13}$
30	600	1.1×10^{17}	$> 10^{13}$
10	700	6.4×10^{15}	1.4×10^{16}
30	700	5.0×10^{15}	1.4×10^{16}
10	800	4.5×10^{13}	2.0×10^{16}
30	800	$> 10^{13}$	2.0×10^{16}
10	900	$> 10^{13}$	2.2×10^{16}
30	900	$> 10^{13}$	2.1×10^{16}
30	1000	$> 10^{13}$	1.7×10^{16}

The contribution of the longest-lived component (with lifetime $\tau_3 = 1.52$ ns) in the annihilation spectra for samples annealed at 500°C and 600°C is equal

to 0.78%. This component decreases to 0.41% for the samples annealed in 700°C and 1000°C with simultaneous increase in τ_3 to 2.25 ns. Similar long-lived components were observed previously [11]. We suppose that such components arise from positronium annihilation in small voids created by the aggregations of vacancies. It is possible to relate the lifetime of positronium with the size of the void positronium annihilates in using an empirical formula given in [17]. According to that $\tau_3 = 1.52$ ns corresponds to the void radius 0.24 nm, and $\tau_3 = 0.25$ ns corresponds to the void radius 0.31 nm.

We conclude that annealing of silicon at 700–1000°C leads to generation of V–P complexes and probably to clustering of void-type defects into big size vacancies aggregations mainly at the expense of the population of divacancies, which are dominant type of defects in non-annealed samples of neutron irradiated silicon.

4.2. Resistivity

The resistivity measurements were performed on the irradiated samples annealed at 500–1000°C for 10–30 min in rapid thermal annealing furnace. Resistivity was measured by four-needle probe. The resistivity of the annealed material strongly depends on temperature and duration of the process (Fig. 3). We found that the best conditions for radiation damage annealing was 800°C and 20 min. The resistivity of the annealed NTD samples were $\approx 1\ \Omega$ cm for the samples produced in the 100 h irradiation run and $\approx 3\ \Omega$ cm for the samples irradiated for 42 h. It is evident that the determined resistivities matched the values estimated in Sect. 3 on the basis of the neutron dose [5].

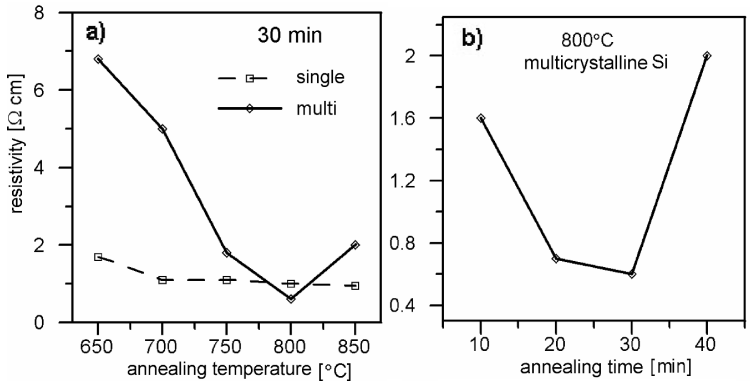

Fig. 3. Dependence of the final resistivity of silicon samples on the temperature (a) and time of annealing (b).

The uniformity of the resistivity distribution in sample annealed at 800°C for 20 min was studied with the bulk photovoltaic effect (BPV) produced by the gradients of resistivity [18]. For comparison, the sample doped during crystallization was studied. The measurements were performed on the 50 mm diameter

samples of $\approx 3\ \Omega$ cm resistivity. The light probe was of 0.2 mm diameter. The amplitude of the fluctuations in the profiles of the BPV voltage are for NTD samples half of those observed in the samples doped during crystallization (Fig. 4). The resistivity variations across sample calculated on the basis of the BPV data for the NTD sample are confined within 2.5% error band (Fig. 5).

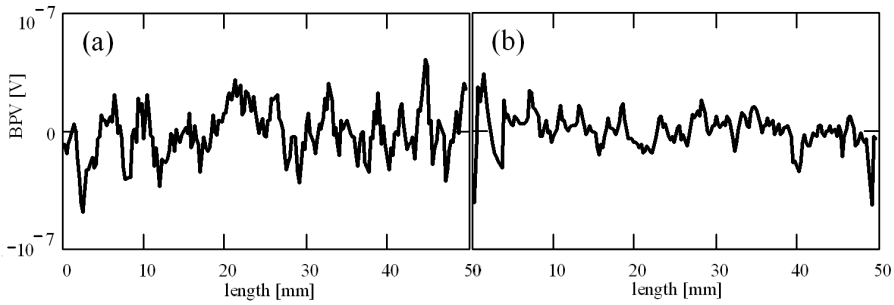

Fig. 4. Profiles of the photoelectric voltage (BPV) along the diameter of the Si wafer measured for the sample doped during crystallization (a) and the sample doped by the neutron transmutation (b).

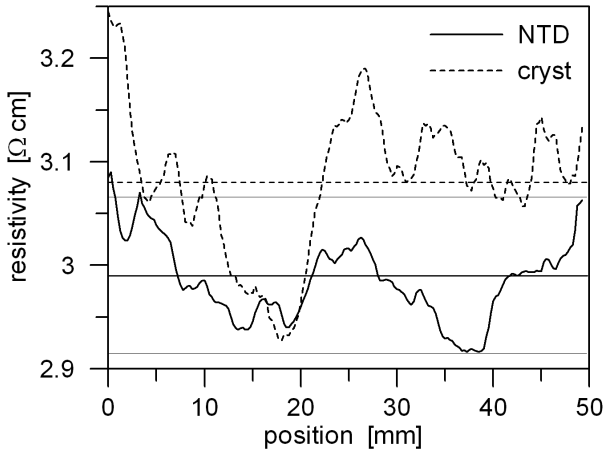

Fig. 5. The spatial distribution of the resistivity along sample diameter determined from BPV data for NTD sample (solid line) and the sample doped during crystallization (dotted line). The horizontal lines denote the average resistivity of each sample. The thin solid lines are $\pm 2.5\%$ error band limits for NTD sample.

4.3. Minority lifetime carrier

Preliminary measurements of the minority carriers' lifetime have been performed with photoconductivity decay technique for the samples studied. The

measurements revealed substantial decrease in minority carrier lifetime to ≈ 1 μs in the NTD samples. It attains only approximately 1% of the minority carrier lifetime value obtained for the material before irradiation. This effect is attributed to high density of radiation defects [19, 20]. It is the main problem in application of neutron doped material in solar cell devices. We hope that the effect can be reduced with application of softer neutrons, i.e. neutrons of lower epithermal index, in irradiation. This can be accomplished by performing irradiation outside the reactor core in the reflector region.

5. Conclusions

Our resistivity studies proved that the nuclear transmutation doping technique provides good uniformity of the irradiated samples. It was confirmed that divacancies are dominant type of defects in the neutron irradiated silicon. Annealing of the samples at 700–1000°C produces V–P complexes generation and void-type defects clustering into big size vacancies aggregations. Since the strong reduction of minority carriers' lifetime is the main problem of the application of NTD material in solar cells, the effect should be studied for different irradiation conditions.

Acknowledgments

This work was partially financed under the Polish Ministry of Science and Higher Education research grants N508 048 31/2569 and N515 08 8433.

References

[1] L.J. Geerlings, P. Manshanden, G.P. Wyers, E.J. Øvrelid, O.S. Raaness, A.N. Waernes, B. Wiersma, in: *Proc. 20th European PV Solar Energy Conf. and Exhibition, Barcelona (Spain) 2005*, Eds. W. Paltz, H. Ossenbrink, P. Helm, Barcelona 2005, p. 619.

[2] D. Sarti, R. Einhaus, *Solar Energy Mater. Solar Cells* **72**, 27 (2002).

[3] A. Cuevas, *Mater. Forum* **27**, 1 (2004).

[4] W.R. Runyan, *Silicon Semiconductor Technology*, McGraw-Hill Book Company, New York 1965.

[5] N.W. Crick, H. Blowfield, in: *Silicon Transmutation Doping Techniques and Practice, IAEA-TECDOC-456*, IAEA, Vienna 1988, p. 65.

[6] J. Kansy, *Nucl. Instrum. Methods Phys. Res. A* **374**, 235 (1996).

[7] W. Brandt, R. Paulin, *Phys. Rev. B* **5**, 2430 (1972).

[8] R. Krause-Rehberg, H.S. Leipner, *Positron Annihilation in Semiconductors, Defect Studies, Springer Series in Solid State Science*, Springer, Berlin 1999.

[9] X.T. Meng, A.K. Liolios, M. Chardalas, Sp. Dedoussis, C.A. Eleftheriadis, Stef. Charalambous, *Phys. Lett. A* **157**, 73 (1991).

[10] W. Puff, X.T. Meng, *J. Appl. Phys.* **73**, 648 (1993).

[11] M. Coeck, N. Balcaen, T. Van Hoecke, B. Van Waeyenberge, D. Segers, C. Dauwe, C. Laermans, *J. Appl. Phys.* **87**, 3674 (2000).

[12] M. Hasegawa, T. Chiba, A. Kawasuso, T. Akahane, M. Suezawa, S. Yamaguchi, K. Sumino, *Mater. Sci. Forum* **196-201**, 1481 (1995).

[13] A. Kawasuso, M. Hasegawa, M. Suezawa, S. Yamaguchi, K. Sumino, *Hyperfine Interact.* **84**, 397 (1994).

[14] A. Polity, F. Börner, S. Huth, S. Eichler, R. Krause-Rehberg, *Phys. Rev. B* **58**, 10363 (1998).

[15] R. Krause-Rehberg, G. Dlubek, A. Polity, *Mater. Sci. Forum* **196-201**, 1649 (1995).

[16] A. Kawasuso, M. Hasegawa, M. Suezawa, S. Yamaguchi, K. Sumino, *Jpn. J. Appl. Phys. Pt. 1* **34**, 2197 (1995).

[17] M. Eldrup, D. Lightbody, J.N. Sherwood, *Chem. Phys.* **63**, 51 (1981).

[18] S. Sikorski, T. Piotrowski, *Progr. Quant. Electron.* **27**, 295 (2003).

[19] G.C. Messenger, M.S. Ash, *The Effects of Radiation on Electronic Systems*, Van Nostrand Reinhold, New York 1992.

[20] G.C. Messenger, *IEEE Trans. Nucl. Sci.* **39**, 468 (1992).